EUROPEAN SYNCHROTRON RADIATION FACILITY

INSTALLATION EUROPEENNE DE RAYONNEMENT SYNCHROTRON

ESRF

Experiment Report Form

The double page inside this form is to be filled in by all users or groups of users who have had access to beam time for measurements at the ESRF.

Once completed, the report should be submitted electronically to the User Office via the User Portal:
https://wwws.esrf.fr/misapps/SMISWebClient/protected/welcome.do

Deadlines for submission of Experimental Reports

Experimental reports must be submitted within the period of 3 months after the end of the experiment.

Experiment Report supporting a new proposal ("relevant report")

If you are submitting a proposal for a new project, or to continue a project for which you have previously been allocated beam time, you must submit a report on each of your previous measurement(s):

- even on those carried out close to the proposal submission deadline (it can be a *"preliminary report"),*
- even for experiments whose scientific area is different form the scientific area of the new proposal,
- carried out on CRG beamlines.

You must then register the report(s) as "relevant report(s)" in the new application form for beam time.

Deadlines for submitting a report supporting a new proposal

- 1st March Proposal Round - **5th March**
- 10th September Proposal Round - **13th September**

The Review Committees reserve the right to reject new proposals from groups who have not reported on the use of beam time allocated previously.

Reports on experiments relating to long term projects

Proposers awarded beam time for a long term project are required to submit an interim report at the end of each year, irrespective of the number of shifts of beam time they have used.

Published papers

All users must give proper credit to ESRF staff members and proper mention to ESRF facilities which were essential for the results described in any ensuing publication. Further, they are obliged to send to the Joint ESRF/ ILL library the complete reference and the abstract of all papers appearing in print, and resulting from the use of the ESRF.

Should you wish to make more general comments on the experiment, please note them on the User Evaluation Form, and send both the Report and the Evaluation Form to the User Office.

Instructions for preparing your Report

- fill in a separate form for each project or series of measurements.
- type your report in English.
- include the experiment number to which the report refers.
- make sure that the text, tables and figures fit into the space available.
- if your work is published or is in press, you may prefer to paste in the abstract, and add full reference details. If the abstract is in a language other than English, please include an English translation.

ESRF	**Experiment title:** XRD characterization of Pt structural properties and its correlation with spin orbit interaction in magnetic epitaxial stacks	**Experiment number**: HC-4764
Beamline: BM25	**Date of experiment**: from: 3rd March to: 7th March	**Date of report**: 26/05/2022
Shifts: 12	**Local contact(s)**: Juan Rubio Zuazo	*Received at ESRF:*

Names and affiliations of applicants (* indicates experimentalists):

Iciar Arnay*, **Adrián Gudín***, Rubén Guerrero, Paolo Perna, Julio Camarero

IMDEA Nanoscience institure, C/Faraday 9 28049 Madrid, Spain

Alberto Anadón*

Institut Jean-Lagmoir, Campus Artem, 2 allée André Guinier, 54011 Nancy, France

Report:

Proposal summary and main objectives: The aim of the proposal was to characterized by means of X-Ray diffraction (XRD) the structural properties of epitaxial Co(111)/Pt(111) bilayer prepared onto (0001)-oriented Al_2O_3 substrates and capped by Al. The structural properties of the Pt layer are related with its efficiency of charge to spin interconversionWe have characterized this interconversion by spin torque ferromagnetic resonance (ST-FMR), spin pumping FMR (SP-FMR) and Spin Seebeck measurements along different crystallographic directions. Pt is one of the most effective materials in terms of spin current generation, being therefore of huge technological interest. Nevertheless, the role of the cristallographic direction in the spin conversion is still under debate,as is demonstrated by the wide range of spin generation efficiency values experimentally obtained by different techniques in the same material. It appears that in such systems the role of the metal/ferromagnet interface is as important as the bulk material due the Rashba-Bishkoff spin orbit coupling. Thus, although the promising technological perspectives, the control of the spin generation remains under study and the real efficiency of crystalline Pt for spin generation is still unknown. Through this thoughtful structural study, and combining it with mentioned ST-FMR, SP-FMR and SSE measurementswe aimed at understanding the relation between the crystalline structure of Pt and its efficiency for spin current generation.

Experiment results: For this experiment we were granted 12 shifts of beam time, which was enough to characterize our set of samples. We performed XRD diffraction measurements in Co/Pt(111) stacks with different Pt thickness (t_{Pt}=5, 10, 15 and 20 nm) and a fixed Co thickness of 5 nm. The experiment was performed at the Grazing incidence x-ray diffraction experimental station at ambient conditions, taking advantage of access to a wide section of the reciprocal space. The complete set of measurements included low angle reflectivity, θ–2θ scans in symmetric and asymmetric geometries, 360 rocking scans around Pt and Co reflections and rods at different substrate position. Additionally, reciprocal space maps (RSM) were recorded, taking advantage of the bidimensional detector installed at the beamtime. An incident angle of 0.5 degrees and a beam energy of 25 keV (λ=0.4954 Å) was used. Figure 1 summarized the structural characterization performed during the experiment in Co/Pt(111) bilayers with different Pt thickness.

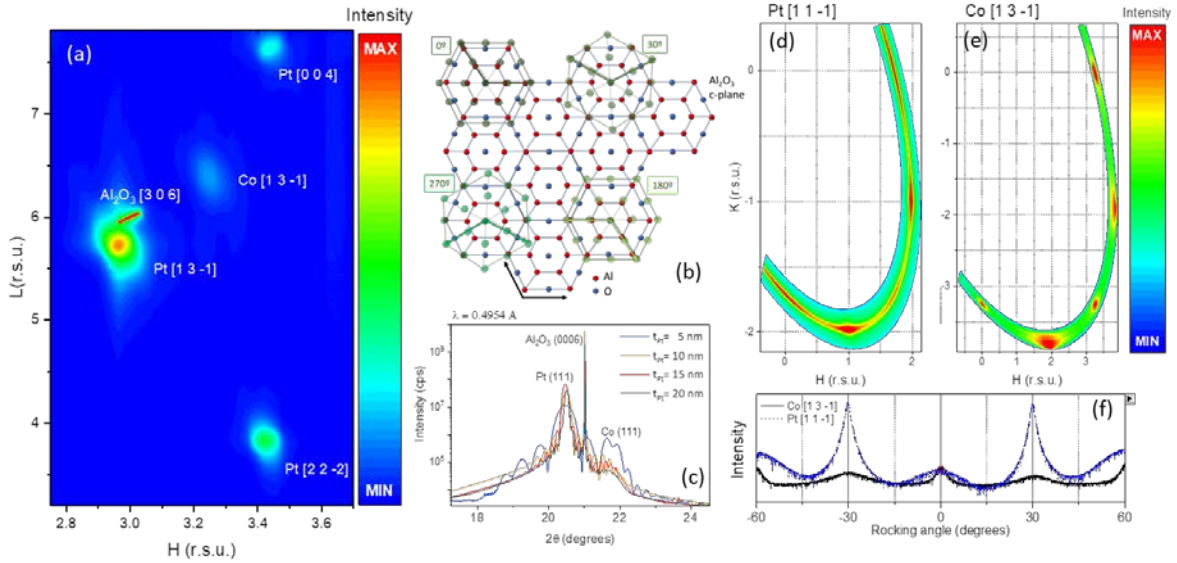

Figure 1: a) RSM around Al_2O_3[306], Pt[1$\bar{3}$1] and Co[13$\bar{1}$]. Additional Pt[004] and Pt[22$\bar{2}$] reflections are observed due to the presence of domains rotated 30 degrees. B) Schematic image of Pt/Al_2O_3 lattice coupling. C) θ-2θ scans around surface normal. D) and e) show bidimensional RSM of rocking curves around Pt[11$\bar{1}$] and Co [13$\bar{1}$] respectively. F) linear representation of d) and e) curves.

The results proved the growth of completely (111)-textured Pt and Co films. Considering in-plane structural properties, we observed a high degree of mosaicity, so that intensity never dissapears when rocking the sample around different crystallographic axis although maximum intensity is observed for certain angles. Main preferential direction corresponds with a 30 degrees rotation so that lattice mismatch between the substrate an the Pt film is minimized. Second family of reflections corresponds with an axis-on-axis growth. The Co film grows axis-on-axis on Pt, translating the same symmetry and crystallographic properties of the Pt film. Thus, the following epitaxial relations are observed: $Al_2O_3[11\bar{2}0]||Pt[01\bar{1}]||Co[[01\bar{1}]$ (0º), $Al_2O_3[11\bar{2}0]||Pt[11\bar{2}]||Co[[11\bar{2}]$ (30º), $Al_2O_3[11\bar{2}0]||Pt[0\bar{1}1]||Co[0\bar{1}1]$ (180º) and $Al_2O_3[11\bar{2}0]||Pt[\bar{1}\bar{1}2]||Co[[\bar{1}\bar{1}2]$ (210º). The appearance of Kiessig fringes even at high diffraction angle indicates the formation of extremely flat interfaces, which favors the coupling between both structures. The high in-plane mosaicity of the films indicates a relaxed growth of Pt and Co structrures, presenting a bulk-like lattice parameter.

Relation with the previous work: In order to unravel the dependence between spin to charge interconversion efficiency in Pt and crystallographic directions, identical samples were processed by standard optical lithography. Microscope images of patterned Co/Pt slabs for the two crystallographic directions are shown in figure 2a. In order to perform SP-FMR measurements, a coplanar waveguide (CPW) antenna is integrated in the last step of lithography and insulated from the sample by a SiO_2 200 nm capping layer. During the measurement a GHz radio-frequency (rf) current is injected in antenna, which generates a rf field (h_{rf}) along the long axis of the sample, while a static in-plane magnetic field (H_{dc}) is also applied parallel to the crystallographic direction chosen. The precession of the magnetization leads to the creation of a pure transverse spin current J_S that is injected from the Co to the Pt layer. Due to the inverse spin hall effect (ISHE), the spin current is converted into a charge current in the Pt and detected by measuring the output voltage. Figure 2b shows the voltage owing to spin pumping mesured as a function of the applied magnetic field at different frequencies for the sample with a 20 nm thick Pt layer.

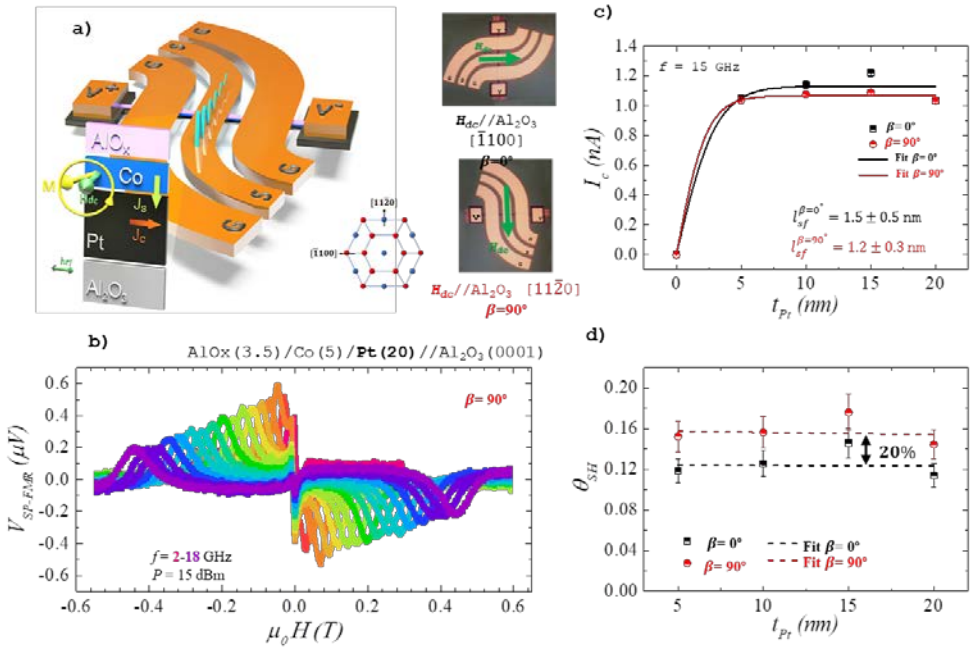

Figure 2: a) Schematic diagram of SP-FMR measurements of AlOX(3.5 nm)/Co(5 nm) Pt(t_{Pt})// Al2O3(0001). Right insets are optical microscope images of patterned Co/Pt slabs with an insulator cap SiO2 (200 nm) and an antenna deposited on top for the two crystallographic directions in which the Hdc is applied. b) Spin pumping voltage for AlOx(3.5 nm)/Pt(20 nm)/Co(5 nm)// Al2O3(0001) at β=90° with f =2- 18 GHz at P = 15 dBm. c) Produced charge current (Ic) as a function of the Pt thickness (t_{Pt}) for 15 GHz at the two orthogonal crystallographic directions. d) Pt-Thickness dependence of the charge-to-spin conversion efficiency measured in epitaxial Pt.

By these experiments we determined the resonant magnetic field (H_{res}), the linewidth (ΔH) and the spin pumping voltage ($V_{SP\text{-}FMR}$). Consequently, we obtained the effective saturation magnetization (M_{eff}), the Gilbert magnetic damping (α) and the charge current (I_C) of the stack. Figure 2c shows the evolution of the charge current produced along Al_2O_3 [$\bar{1}$100] and Al_2O_3 [11$\bar{2}$0] directions, corresponding mainly to Pt [1$\bar{1}$0]/Pt[$\bar{1}$10] and Pt[11$\bar{2}$]/Pt[$\bar{1}\bar{1}$2] non equivalent directions. By fitting the data, the spin diffusion length can be extracted, showing values of 1.5±0.5 nm and 1.2±0.3 nm for Al_2O_3 [$\bar{1}$100] and Al_2O_3 [11$\bar{2}$0] directions respectively. The results are in agreement with previous reports in the literature [1] and do not reveal significant differences between both crystallographic axis. Nevertheless, when analyzing the evolution of the spin hall angle (θ_{SH}), as shown in figure 2d, an anisotropic behavior between the two crystallographic directions nearly to 20% can be clearly appreciated. This parameter was obtained considering the effective spin current flowing in the Pt layer by the following relation:

$$I_C = \frac{V_{SP-FMR}}{R} = w l_{sf}^{Pt} \theta_{SH} J_S^{eff} \tanh\left(\frac{t_{Pt}}{2 l_{sf}^{Pt}}\right) \quad (1)$$

where w=10 μm is the width of the device, J_S^{eff} is the effective spin current density, l_{sf}^{Pt} is the spin diffusion length and θ_{SH} the effective spin Hall angle. Thus, θ_{SH} =0.158 ± 0.02 and 0.124 ± 0.02 values are estimated from (1) for Al_2O_3 [1-100] and Al_2O_3 [11-20] directions respectively. These values correlate fairly well with previous results in the literature for high spin hall angles in FM/Pt bilayers [3] and further support the recently published study[2] that the anisotropy arises due to the specific crystallographic orientation of epitaxial Pt.

References

[1]C. T. Bonne *et al.* J. Appl. Phys. 113, 153906 (2013), O. Mosendz *et al.* Phys. Rev. B. 82, 214403 (2010)
[2] W. Zhang *et al.* Nat. Phys. 11(6), 496-502 (2015), M. Obstbaum *et al.* Phys. Rev. B 89, 060407 (2014)
[3] R. Thompson *et al.* Phys. Rev. Appl. 15, 014055 (2021); Q. Bai *et al.* Appl. Phys. Lett. 118, 132403 (2021)